medRxiv preprint doi: https://doi.org/10.1101/2020.07.02.20144212; this version posted October 7, 2020. The copyright holder for this preprint (which was not certified by peer review) is the author/funder, who has granted medRxiv a license to display the preprint in perpetuity.
It is made available under a CC-BY-NC-ND 4.0 International license .

1 **Main Manuscript for**

2 Transfer RNA fragments replace microRNA regulators of the 3 cholinergic post-stroke immune blockade

4 Short title: tRF/miR balancers of post-stroke immunity

5

6 Katarzyna Winek†[1,2], Sebastian Lobentanzer†[3], Bettina Nadorp[1,4], Serafima Dubnov[1,2], Claudia 7 Dames[5], Sandra Jagdmann[5], Gilli Moshitzky[1], Benjamin Hotter[6], Christian Meisel[5], David S 8 Greenberg[2], Sagiv Shifman[7], Jochen Klein[3], Shani Shenhar-Tsarfaty[8], Andreas Meisel[6], Hermona 9 Soreq*[1,2]

10 †these authors contributed equally;

11 [1] The Edmond & Lily Safra Center for Brain Sciences, The Hebrew University of Jerusalem, 12 Jerusalem, Israel

13 [2] The Alexander Silberman Institute of Life Sciences, The Hebrew University of Jerusalem, 14 Jerusalem, Israel.

15 [3] Department of Pharmacology, College of Pharmacy, Goethe University, Frankfurt am Main, 16 Germany

17 [4] The Grass Center for Bioengineering, Benin School of Computer Science and Engineering, 18 The Hebrew University of Jerusalem, Jerusalem, Israel.

19 [5] The Institute for Medical Immunology, Charité-Universitätsmedizin Berlin, Germany.

20 [6] NeuroCure Clinical Research, Center for Stroke Research Berlin and The Department 21 of Neurology, Charité-Universitätsmedizin Berlin, Germany

22 [7] The Department of Genetics, The Hebrew University of Jerusalem, Jerusalem, Israel.

23 [8] Department of Internal Medicine "C", "D" and "E", Tel Aviv Sourasky Medical Center and 24 Sackler Faculty of Medicine, Tel Aviv University, Tel Aviv, Israel.

25

26 *to whom correspondence should be addressed at hermona.soreq@mail.huji.ac.il;

27 Edmond J. Safra Campus Givat Ram, 91904 Jerusalem, Israel +972 54 882 0629

NOTE: This preprint reports new research that has not been certified by peer review and should not be used to guide clinical practice.

medRxiv preprint doi: https://doi.org/10.1101/2020.07.02.20144212; this version posted October 7, 2020. The copyright holder for this preprint (which was not certified by peer review) is the author/funder, who has granted medRxiv a license to display the preprint in perpetuity.
It is made available under a CC-BY-NC-ND 4.0 International license .

28 ORCID IDs:
29 Katarzyna Winek 0000-0003-3085-9054
30 Sebastian Lobentanzer - 0000-0003-3399-6695
31 Bettina Nadorp 0000-0003-1974-8425
32 Serafima Dubnov 0000-0001-7982-6195
33 Claudia Dames 0000-0002-9030-9532
34 Sandra Jagdmann 0000-0003-4909-0281
35 Gilli Moshitzky 0000-0002-9740-1593
36 Benjamin Hottter 0000-0002-5272-9181
37 Christian Meisel 0000-0003-0222-991X
38 David S. Greenberg 0000-0001-8959-8640
39 Sagiv Shifman 0000-0003-4071-5361
40 Jochen Klein - 0000-0001-6971-3381
41 Shani Shenhar-Tsarfaty 0000-0002-8268-1799
42 Andreas Meisel 0000-0001-7233-5342
43 Hermona Soreq - 0000-0002-0955-526X
44
45
46

medRxiv preprint doi: https://doi.org/10.1101/2020.07.02.20144212; this version posted October 7, 2020. The copyright holder for this preprint (which was not certified by peer review) is the author/funder, who has granted medRxiv a license to display the preprint in perpetuity.
It is made available under a CC-BY-NC-ND 4.0 International license .

47

48 **Classification**

49 Biological Sciences: Medical Sciences

50 **Keywords**

51 acetylcholine; ischemic stroke; microRNA; immunology; transfer RNA fragment

52 **Author Contributions**

53 K.W and S.L. analyzed and interpreted RNA-sequencing data and wrote the manuscript, S.L.
54 conducted bioinformatic analyses, B.N. and S.S-T. processed the blood samples and prepared
55 the sequencing data, S.D. and K.W. established tRF size selection protocols and performed the
56 RT-qPCR measurements, K.W. performed the cell culture tests, G.M. contributed to sequencing
57 analyses, A.M., B.H., C.M. collected the stroke cohort, the blood samples and performed
58 immunological measurements; C.D. and S.J. performed experiments with human monocytes and
59 immunological measurements, D.S.G, S.S. and J.K. interpreted data and edited the manuscript;
60 H.S. and A.M. co-guided the project, planned the experiments, interpreted data and edited the
61 manuscript; all co-authors read and commented on the manuscript contents.

62

63 **Abstract**

64 Stroke is a leading cause of death and disability. Recovery depends on a delicate balance
65 between inflammatory responses and immune suppression, tipping the scale between brain
66 protection and susceptibility to infection. Peripheral cholinergic blockade of immune reactions
67 fine-tunes this immune response, but its molecular regulators are unknown. Here, we report a
68 regulatory shift in small RNA types in patient blood sequenced two days after ischemic stroke,
69 comprising massive decreases of microRNA levels and concomitant increases of transfer RNA
70 fragments (tRFs) targeting cholinergic transcripts. Electrophoresis-based size-selection followed
71 by RT-qPCR validated the top 6 upregulated tRFs in a separate cohort of stroke patients, and
72 independent datasets of small and long RNA sequencing pinpointed immune cell subsets pivotal
73 to these responses, implicating CD14$^+$ monocytes in the cholinergic inflammatory reflex. In-depth
74 small RNA targeting analyses revealed the most-perturbed pathways following stroke and implied
75 a structural dichotomy between microRNA and tRF target sets. Furthermore, lipopolysaccharide
76 stimulation of murine RAW 264.7 cells and human CD14$^+$ monocytes upregulated the top 6
77 stroke-perturbed tRFs, and overexpression of stroke-inducible tRF-22-WE8SPOX52 using an
78 ssRNA mimic induced downregulation of immune regulator Z-DNA binding protein 1 (Zbp1). In
79 summary, we identified a “changing of the guards” between RNA types that may systemically
80 affect homeostasis in post-stroke immune responses, and pinpointed multiple affected pathways,
81 which opens new venues for establishing therapeutics and biomarkers at the protein- and RNA-
82 level.

83 **Significance Statement**

84 Ischemic stroke triggers peripheral immunosuppression, increasing the susceptibility to post-
85 stroke pneumonia that is linked with poor survival. The post-stroke brain initiates intensive
86 communication with the immune system, and acetylcholine contributes to these messages; but
87 the responsible molecules are yet unknown. We discovered a “changing of the guards,” where
88 microRNA levels decreased but small transfer RNA fragments (tRFs) increased in post-stroke
89 blood. This molecular switch may re-balance acetylcholine signaling in CD14$^+$ monocytes by

medRxiv preprint doi: https://doi.org/10.1101/2020.07.02.20144212; this version posted October 7, 2020. The copyright holder for this preprint (which was not certified by peer review) is the author/funder, who has granted medRxiv a license to display the preprint in perpetuity.
It is made available under a CC-BY-NC-ND 4.0 International license .

90 regulating their gene expression and modulating post-stroke immunity. Our observations point out
91 to tRFs as molecular regulators of post-stroke immune responses that may be potential
92 therapeutic targets.
93
94 **Main Text**
95
96 **Introduction**
97
98 Stroke is a global burden of growing dimensions, accounting for ca. 5.5 million deaths annually,
99 and leaving most of the surviving patients permanently disabled (1). The immune system is one
100 of the main players in the pathophysiology of stroke. Brain injury dampens immune functions in
101 the periphery, which limits the inflammatory response and infiltration of immune cells into the
102 CNS and may pose a neuroprotective mechanism in stroke patients. However, this systemic
103 immunosuppression simultaneously increases the risk of infectious complications (2), e.g. by
104 inducing lymphocyte apoptosis and decreasing the production of pro-inflammatory cytokines
105 (lymphocytic IFNγ and monocytic TNFα) (3). Therefore, post-stroke recovery largely depends on
106 a delicate balance between inflammation, which exacerbates the severity of symptoms, and the
107 post-stroke suppression of immune functions, which increases the susceptibility to infections (3).
108 This involves incompletely understood molecular regulator(s) of cholinergic and sympathetic
109 signaling and the hypothalamus-pituitary-adrenal gland axis (HPA). Among other processes,
110 brain injury leads to activation of the vagus nerve, which mediates anti-inflammatory signaling
111 through the cholinergic efferent fibers and the noradrenergic splenic nerve (4). Binding of
112 acetylcholine (ACh) to the nicotinic alpha 7 receptors on monocytes/macrophages decreases the
113 production of proinflammatory cytokines (4, 5) in a manner susceptible to suppression by
114 microRNA (miR) regulators of cholinergic signaling, such as miR-132 (6). We hypothesized that
115 this and other small RNA fine-tuners of innate immune responses, including miRs and the
116 recently re-discovered transfer RNA (tRNA) fragments (tRFs), may contribute to regulation of
117 post-stroke processes.
118
119 Both miRs and tRFs may control entire biological pathways, such that their balanced
120 orchestration could modulate brain-induced systemic immune functioning. miRs are small non-
121 coding RNAs whose expression requires transcription yet can be rapidly induced, enabling
122 degradation and/or translational suppression of target genes carrying a complementary motif.
123 One miR may suppress the expression of many targets involved in the same biological pathway,
124 and many miRs may co-target the same transcripts, enabling cooperative suppression. Hence,
125 miR regulators of ACh signaling may regulate the role of ACh in both cognitive function and
126 systemic inflammation (6, 7).
127 Recent reports highlight tRNA as another major source of small noncoding RNA(8), including
128 tRNA halves (tiRNAs) and smaller tRNA fragments - tRFs. tiRNAs are created by angiogenin
129 cleavage at the anticodon loop (9) raising the possibility that the post-stroke angiogenin increase
130 might change their levels (10). Among other functions (11, 12), smaller fragments derived from
131 the 3'- or 5'-end of tRNA (3'-tRF/5'-tRF) or internal tRNA parts (i-tRF) may incorporate into
132 Argonaute (Ago) protein complexes and act like miRs to suppress their targets (13). Differential
133 expression of tRFs was reported under hypoxia, oxidative stress, ischemic reperfusion (9, 14)
134 and in epilepsy (15), which are all involved in ischemic stroke complications. tRFs may be
135 generated via enzymatic degradation of tRNA, independent of de-novo transcription, which
136 implies that tRF levels may be modulated more rapidly than miR levels. However, whether brain-
137 body communication and immune suppression after ischemic stroke in human patients involves
138 blood tRF changes has not yet been studied.
139
140 Taking into consideration that the cholinergic system is one of the controllers of immune
141 functions, we investigated changes in the levels of miR- and tRF-regulators, with a specific focus
142 on those which may control the ACh-mediated suppression of post-stroke immune functions. We
143 performed small and long RNA-sequencing of whole blood samples collected from ischemic

medRxiv preprint doi: https://doi.org/10.1101/2020.07.02.20144212; this version posted October 7, 2020. The copyright holder for this preprint (which was not certified by peer review) is the author/funder, who has granted medRxiv a license to display the preprint in perpetuity.
It is made available under a CC-BY-NC-ND 4.0 International license .

144 stroke patients two days after stroke onset, mined RNA-sequencing datasets of blood cell
145 transcripts and sought potential links between perturbed miRs and tRFs, post-stroke immune
146 responses and the cholinergic anti-inflammatory pathway.
147
148
149 **Results**
150
151 **Stroke-perturbed small RNAs display a cholinergic-associated shift from miRs to tRFs**
152 To seek post-stroke small RNA regulators of body-brain communication, we first performed small
153 RNA-sequencing of whole blood samples collected on day 2 after ischemic stroke from 33 male
154 patients of the PREDICT cohort (484 participants) (16) and 10 age- and sex-matched controls
155 (Fig. 1A; see demographic data in Data file S1). Principal Component Analysis (PCA) of the
156 differentially expressed (DE) small RNAs completely segregated the stroke and control groups
157 (Fig. 1B). The respective direction of change among the two small RNA classes involved a
158 statistically significant decline in miRs and a parallel increase in tRFs, indicating a 'changing of
159 the guards' from miRs to tRFs. Specifically, 87% of the 143 DE tRFs were upregulated, whereas
160 63% of the 420 DE miRs were downregulated (Benjamini-Hochberg corrected $p < 0.05$; Fig.
161 1C&D). Of the 143 DE tRFs, 87 were 3'-tRFs, and 30 of those (all upregulated) were derived from
162 alanine binding tRNA (Fig. S1), indicating non-arbitrary fragment generation.
163 Notably, the 420 DE miRs included several miRs known to be perturbed in stroke: hsa-miR-532-
164 5p (logFC = -2.27, p = 1.81e-33) (17), hsa-miR 148a-3p (logFC = -2.30, p = 9.61e-19) and hsa-
165 let-7i-3p (logFC = -1.07, p = 4.31e-04) (18). To test the potential involvement of miRs and tRFs in
166 regulating the cholinergic anti-inflammatory pathway after stroke, we performed targeting analysis
167 of DE miRs and tRFs towards cholinergic transcripts (Supplementary Methods, for a complete list
168 of cholinergic genes see Data File S2) via an in-house integrative database (*miRNeo*) (19)
169 containing comprehensive transcription factor (TF)- and miR-targeting data, complemented by
170 de-novo prediction of tRF-targeting using TargetScan (20). A restrictive approach identified 131
171 miRs and 64 tRFs containing complementary motifs to at least five cholinergic-associated
172 transcripts each (further termed "Cholino-miRs" and "Cholino-tRFs", Fig. 1C&D, Fig. S2, full lists
173 in Data files S3 and S4). Permutation targeting analysis showed an enrichment of cholinergic
174 targets for both DE miRs (100 000 permutations, p = 0.0036) and DE tRFs (100 000
175 permutations, p = 2e-05). Further indicating non-random generation of these fragments, the tRFs
176 identified in our dataset clustered into oligonucleotide families with high sequence homology via t-
177 distributed stochastic neighbor embedding (t-SNE) (Fig. 1E), including families known to
178 associate with Ago and suppress growth and proliferation via post-transcriptional downregulation
179 in lymphocytes (e.g. tRF-22-WE8SPOX52 from tRNAGly) (21) and metastatic cancer cells (tRF-
180 18-HR0VX6D2 from tRNALeu) (22). This supported our prediction that the concomitant elevation
181 of tRF- and decline of miR-levels in post-stroke blood could contribute to the post-stroke changes
182 in cholinergic signaling pathways.
183
184 **Figure 1. Post-stroke differential expression of small RNA species and tRF homology**
185 **clustering.** A) Whole blood total RNA were collected on day 2 post-stroke from patients of the
186 PREDICT cohort (NCT01079728) (16) and age-matched controls. B) PCA of DE tRFs/miRs in
187 patients' blood separated stroke and control samples. C) Volcano plot of DE tRFs from stroke
188 patients and controls (horizontal line at adjusted p = 0.05) showing upregulation of most DE tRFs.
189 D) Volcano plot of DE miRs shows predominant downregulation in stroke patients compared with
190 controls (horizontal line at adjusted p = 0.05). Red dots in C and D reflect Cholino-tRFs and
191 Cholino-miRs, respectively. E) t-SNE visualization of tRF homology based on pairwise alignment
192 scores of sequences of all detected tRNA fragments shows grouped tRFs of several specific
193 amino acid origins.

194 To further challenge our findings, we validated the expression levels of prominently DE tRFs
195 identified by RNA sequencing in a separate cohort of PREDICT patients (16). Standard qPCR
196 techniques cannot distinguish between the full length tRNA molecules and their 3'-tRF cleavage

medRxiv preprint doi: https://doi.org/10.1101/2020.07.02.20144212; this version posted October 7, 2020. The copyright holder for this preprint (which was not certified by peer review) is the author/funder, who has granted medRxiv a license to display the preprint in perpetuity.
It is made available under a CC-BY-NC-ND 4.0 International license .

197 products. Therefore, to experimentally validate tRF changes (Fig. 2A) we implemented an
198 electrophoresis size selection-based strategy followed by cDNA synthesis from the selected small
199 RNAs and RT-qPCR (maximum 25 nt, Fig. 2B). This procedure validated the top six upregulated
200 tRFs identified in RNA-sequencing data (tRF-22-WEKSPM852, tRF-18-8R6546D2, tRF-18-
201 HR0VX6D2, tRF-18-8R6Q46D2, tRF-22-8EKSP1852 and tRF-22-WE8SPOX52; according to
202 count-change, see Supplementary Methods, Fig. 2B&C) and demonstrated significant increases
203 accompanied by higher variability in the blood levels of these tRFs in post-stroke patients
204 compared to controls.
205
206 **Figure 2. RT-qPCR validation of the top 6 upregulated tRFs in PREDICT stroke patients**
207 **following size selection for small RNA.** A) RNA-sequencing counts normalized to the size of
208 the library (using DESeq2 (23)) of the top 6 upregulated tRFs (from left to right). Asterisks
209 indicate adjusted p-values of Wald test via DESeq2, ** $p < 0.01$, *** $p < 0.001$, shown are box-
210 plots with whiskers minimum to maximum. B) Size selection workflow for validations in a separate
211 sub-group of PREDICT stroke patients (n=32) using the same control group (n=10); C) RT-qPCR
212 validations using normalized expression (hsa-miR-30d-5p, hsa-let7d-5p, hsa-miR-106b-3p and
213 hsa-miR-3615 served as house-keeping transcripts, see Supplementary Methods), relative to the
214 control group (line at mean normalized expression for the control group =1) confirmed
215 upregulation of top 6 DE tRFs identified in RNA-sequencing, one-way ANOVA, ** $p < 0.01$, *** $p <$
216 0.001, box-plots with whiskers minimum to maximum.

217 **Stroke-perturbed whole blood tRFs are biased towards cellular blood compartments**
218 To clarify the distribution of stroke-perturbed tRFs among the immunologically relevant blood cell
219 types, we mined an RNA-sequencing dataset comprising sorted cell populations collected from
220 healthy volunteers: $CD4^+$ T helper cells, $CD8^+$ T cytotoxic cells, $CD56^+$ NK cells, $CD19^+$ B cells,
221 $CD14^+$ monocytes, $CD15^+$ neutrophils, $CD235a^+$ erythrocytes, serum, exosomes, and whole
222 blood (450 samples in total, (24)) (Fig. 3A). Predicting that log-normal distribution of the counts in
223 different samples would point towards biological significance, we categorized all tRFs found in
224 this dataset into present/absent in a specific blood compartment (without introducing a limit for
225 counts, see Methods, Fig. 3B). Two main clusters of specific blood compartments could be
226 identified based on their specific tRF profile: a) monocytes, B-, T-, and NK cells; b) neutrophils,
227 whole blood, serum, exosomes, and erythrocytes (Fig. S3). Further, we distinguished eight tRF
228 sub-clusters, based on the presence/absence of specific tRFs in blood compartments (Fig. 3C),
229 with cluster four comprising molecules expressed specifically in monocytes, B-, T-, and NK cells,
230 and cluster seven consisting of tRFs expressed only in monocytes.
231 Based on this methodology, we conducted a census of small RNA species found intra- vs
232 extracellularly: we detected 1624 distinct intracellular tRFs but only 93 extracellular tRFs; 149 in
233 whole blood, but 1417 in $CD14^+$ monocytes alone. Similarly, we detected 559 distinct intracellular
234 miRs but 145 extracellular miRs; 475 in monocytes alone, and 331 in whole blood. Using the
235 presence/absence measure for analyzing the post-stroke DE tRFs (Fig. 3D, Fig. S4 for the top 20
236 stroke DE tRFs), we detected 77 DE tRFs from the PREDICT dataset as expressed in immune
237 cells (Fig. 3E, a detailed list of tRFs and affiliated clusters in Data File S5), including 10 Cholino-
238 tRFs. Notably, tRFs previously shown to function post-transcriptionally in a miR-like manner (e.g.
239 tRF-22-WE8SPOX52 from tRNAGly (21) and tRF-18-HR0VX6D2 from tRNALeu, alias hsa-miR-
240 1280 (22)) segregated into whole blood, monocyte, T, B- and NK cell compartments rather than
241 into erythrocyte, serum or exosome compartments. Thus, the post-stroke modified tRFs may be
242 functionally involved in regulating the leukocytic post-stroke response.
243
244 **Figure 3. Immune cell tRF expression clustering and cell type-specific analysis.** A)
245 Analysis of RNA-sequencing datasets from T lymphocytes ($CD4^+$ T helper cells and $CD8^+$ T
246 cytotoxic cells), B lymphocytes ($CD19^+$), NK cells ($CD56^+$), monocytes ($CD14^+$), neutrophils
247 ($CD15^+$) erythrocytes ($CD235a^+$), serum, exosomes, and whole blood (24) yielded a blood tRF
248 profile. B) Definition of presence/absence of small RNAs in these blood compartments via
249 statistical assertion of log-normal count distribution (values between 0 and 1, closer to 1:

medRxiv preprint doi: https://doi.org/10.1101/2020.07.02.20144212; this version posted October 7, 2020. The copyright holder for this preprint (which was not certified by peer review) is the author/funder, who has granted medRxiv a license to display the preprint in perpetuity.
It is made available under a CC-BY-NC-ND 4.0 International license .

250 present). C) Detailed analysis of identified tRFs found 8 sub-clusters based on cell types
251 expressing specific molecules. D) t-SNE of all found tRFs represented by grey dots, DE tRFs
252 identified in the PREDICT study are marked with cluster-specific color. E) t-SNE of all tRFs found,
253 Cholino-tRFs identified in the PREDICT study are marked with cluster-specific color.

254 **CD14$^+$ monocytes show highest cholinergic-related transcriptional repertoire**

255 The enrichment of DE Cholino-miRs and Cholino-tRFs identified in the PREDICT dataset and the
256 contribution of the cholinergic anti-inflammatory pathway to peripheral immunosuppression called
257 for pinpointing the immune compartment(s) in which these small RNAs might affect post-stroke
258 immune suppression. Analysis of long RNA regulatory circuits (25) specific to blood-borne
259 leukocytes (Fig. 4A) identified CD14$^+$ monocytes as the main cell type expressing cholinergic
260 core and receptor genes (Data File S2, Fig. 4B). To confirm the relevance of this effect, we
261 performed long RNA-sequencing in blood samples from 20 stroke patients from the PREDICT
262 study and 4 controls. This showed 204 upregulated and 490 downregulated long RNA transcripts.
263 Gene ontology (GO) enrichment analyses of the most implicated genes yielded highly specific
264 terms relevant to innate immunity, vascular processes, and cholinergic links (Fig. 4C, list of all
265 significant terms in Table S1). More specifically, terms linked to innate immune processes in post-
266 stroke blood involved responses to LPS mediated by interferons and other cytokines (Fig. 4C,
267 left-hand side); vascular processes comprised platelet activation and degranulation, control of
268 cell-cell adhesion, and regulation of angiogenesis (Fig. 4C, right-hand side). Intriguingly,
269 differentially regulated genes also showed involvement in response to organophosphorus agents,
270 which are known acetylcholinesterase (AChE) inhibitors, supporting a cholinergic participation.
271

272 **Figure 4. Immune cell gene expression clustering and long RNA pathways perturbed in**
273 **stroke blood.** A) Published cell type-specific long RNA profiles (25) were used to visualize
274 transcriptomes of T lymphocytes (CD4$^+$ T-helper cells and CD8$^+$ T-cytotoxic cells), B lymphocytes
275 (CD19$^+$), NK cells (CD56$^+$), monocytes (CD14$^+$), and neutrophils (CD15$^+$). B) t-SNE visualization
276 of 15032 genes on the basis of their expression in blood-borne immune cells extrapolated from
277 transcriptional activities in regulatory circuits (25). Genes are colored by the cell type in which
278 their expression was highest. Cholinergic core and receptor genes were mainly found in the
279 CD14$^+$ monocytic compartment. C) Enrichment of post-stroke DE genes (log2FC > 1.4) in
280 circulation- and immunity-related pathways, presented as t-SNE of GO terms by their shared
281 genes (see Supplementary Methods); color denotes t-SNE cluster, size denotes number of
282 significant genes in term; deeper color indicates lower enrichment p-value (all p-values < 0.05).
283 Distance between terms indicates the number of shared genes between the GO terms, closer
284 meaning more shared genes.

285 **Stroke leads to perturbation of microRNA regulatory networks**

286 Notably, miRs upregulated after stroke both appear in smaller numbers compared to
287 downregulated miRs and possess significantly fewer gene targets per individual miR (via
288 *miRNeo*, mean [up vs down] 463 vs 804, median 266 vs 717, one-way ANOVA $p = 2.1e-07$,
289 $F(1,352) = 28.06$). To unravel target genes of these two miR populations, we performed gene
290 target enrichment via permutation inside *miRNeo* (10,000 permutations). Significantly enriched
291 gene targets (permutation p-value < 0.05) were subjected to GO analyses and visualized in a t-
292 SNE projection, yielding 13 clusters of related terms, indicating most-affected pathways (Fig. 5A,
293 Fig. S5). Within each cluster, we determined the most relevant genes via hypergeometric
294 enrichment (Fisher's exact test). Ranking of the clusters by the absolute number of enriched
295 genes (Benjamini-Hochberg adjusted $p < 0.05$) revealed the putative biological processes that
296 were most influenced by the miR perturbation following ischemic stroke in our patients (Fig. 5B).

297 The significantly de-repressed cluster no. 6 (84 enriched genes) pointed towards perturbation of
298 pathways involved in responses to hypoxia (GO:0036293, p = 0.008) and drugs (GO:0042493, p
299 = 0.035), including antibiotics (GO:0071236, p = 0.013), glucocorticoids (GO:0051384, p =
300 0.007), and the cholinesterase-blocking organophosphorus agents (GO:0046683, p = 0.019),
301 which reinforced the notion of cholinergic participation. Cross-check of enriched genes via DAVID

medRxiv preprint doi: https://doi.org/10.1101/2020.07.02.20144212; this version posted October 7, 2020. The copyright holder for this preprint
(which was not certified by peer review) is the author/funder, who has granted medRxiv a license to display the preprint in perpetuity.
It is made available under a CC-BY-NC-ND 4.0 International license .

302 (26) confirmed a role of cluster no. 6 in hypoxia (GO:0071456, p = 8.3e-13), drug response
303 (GO:0042493, 5.4e-10), and the cholinergic synapse (KEGG pathway 04725, p = 0.006). Cluster
304 no. 8 (with second-most 58 enriched genes) highlighted perturbed transmembrane ion
305 conductivity, particularly in regulation of cardiac muscle cell action (GO:0098901, p = 0.044) and
306 negative regulation of blood circulation (GO:1903523, p = 0.016). DAVID analysis confirmed
307 involvement in '*regulation of cardiac muscle contraction by the release of sequestered calcium*
308 *ion*' (GO:0010881, p = 2.1e-15) and regulation of heart rate (GO:0002027, p = 1.2e-07). The
309 subsequent clusters indicate further involvement in nerve cell regulatory processes (cluster no.
310 4), regulation of gene silencing by miRNA (cluster no. 1), and humoral immunity via IL-1 and IL-6
311 (cluster no. 7) (see also Fig. S5). The entire list of clusters and gene enrichments is available as
312 Data File S6.
313
314 **tRFs may suppress inflammation and cholinergic-associated transcription factors alone or**
315 **in cooperation with miRs**
316 Cellular responses to different stimuli are coordinated by cell type-specific transcriptional
317 regulatory circuits. To facilitate understanding of the role of miRs and tRFs in regulating the
318 transcriptional state of $CD14^+$ monocytes after stroke, we generated a monocyte-specific
319 transcriptional interaction network of small RNAs targeting transcription factors (via *miRNeo*) (19),
320 combined with differential expression of long and small RNAs from the PREDICT cohort. The
321 gradually divergent targeting of these TFs by miRs and/or tRFs implied largely separate domains
322 of regulation by these small RNA species (Fig. 5C). This notion was topologically strengthened by
323 the fact that the force-directed network of all TFs active in $CD14^+$ monocytes self-segregated to
324 form two distinct clusters of TFs which were primarily targeted either by miRs or tRFs, including
325 numerous TFs DE in stroke patient blood (Fig. 5D&E). Among the implied TFs are proteins
326 known for their influence on cholinergic genes as well as their involvement in inflammation, such
327 as STAT1 or KLF4 (27, 28). Notably, 8 DE TFs were not predicted to be targeted by any miR or
328 tRF present in $CD14^+$ monocytes.
329
330 **Figure 5. GO enrichment of miR targets and perturbed pathways; divergent influence of**
331 **miRs and tRFs in $CD14^+$ TF regulatory circuits.** A) t-SNE visualization of GO terms enriched in
332 the targets of miRs perturbed by stroke, performed separately for positively (green) and
333 negatively (red) perturbed miRs, segregated into 13 functional clusters. Size of circles represents
334 the number of genes in the respective GO term; depth of color represents enrichment p-value (all
335 $p < 0.05$). B) Bar graph of clusters identified in *A)* ordered by the number of enriched genes
336 (Fisher's exact test, BH adjusted $p < 0.05$) shows most pertinent processes with miR
337 involvement. C) The top 18 DE TFs in stroke patients' blood present a gradient of targeting by
338 miRs and/or tRFs (left = 100% miR targeting, right = 100% tRF targeting; value shown as "tRF
339 fraction – 0.5" to center on 50/50 regulation by miRs and tRFs). Size of points and color denote
340 absolute count-change and direction of differential regulation, respectively. "C" marks TFs
341 targeting cholinergic core or receptor genes. D) Small RNA targeting of TFs active in $CD14^+$ cells
342 was analyzed using an in-house database (18). E) Force-directed network of all TFs active in
343 $CD14^+$ monocytes self-segregates to form largely distinct TF clusters targeted by DE tRFs and
344 miRs in stroke patients' blood. Yellow = TF, red = TF DE in stroke patients' blood, green = miR,
345 purple = tRF. Size of node denotes activity towards targets.
346
347 **Stroke-induced tRFs show evolutionarily conserved participation in**
348 **macrophage/monocyte responses to inflammatory stimuli**
349 To test if the stroke-induced tRFs are involved in the inflammatory response of monocytes and
350 macrophages, we subjected murine RAW 264.7 cells to LPS-stimulation with or without
351 dexamethasone suppression of their inflammatory reactions (Fig. 6A). By 18h after LPS
352 stimulation, RT-qPCR analysis after size-selection (for ≤50 nt fragments) detected pronounced
353 upregulation of the top 6 post-stroke upregulated tRFs (Fig. 6B). Moreover, dexamethasone
354 suppression of the LPS response led to downregulation of those tRFs, along with a diminished
355 inflammatory response (Fig. S6). Predicted targets of these molecules comprise members of

medRxiv preprint doi: https://doi.org/10.1101/2020.07.02.20144212; this version posted October 7, 2020. The copyright holder for this preprint (which was not certified by peer review) is the author/funder, who has granted medRxiv a license to display the preprint in perpetuity.
It is made available under a CC-BY-NC-ND 4.0 International license .

356 mitogen-activated protein kinases (MAPK) and tumor necrosis factor receptor-associated factors
357 (TRAF) (see Data File S7), further pointing towards their regulatory role in response to
358 inflammatory stimuli. Notably, one of the top 6 stroke-perturbed tRFs, tRF-22-WE8SPOX52, is
359 complementary to the 3`UTR sequence of murine Z-DNA binding protein Zbp1 and therefore a
360 predicted regulator of the Zbp1 transcript and its immune system activity (Fig. 6C). To challenge
361 the functional activity of tRF-22-WE8SPOX52 in murine RAW 264.7 macrophages, we over-
362 expressed this tRF using ssRNA mimics (Fig. 6D, Fig S7), which significantly reduced the
363 expression of its Zbp1 target compared to negative control (NC), as quantified by long RNA
364 sequencing (Fig. 6E) and validated by RT-qPCR in an independent experiment (Fig. 6F).
365
366 Lastly, we aimed to validate the functional implications of these findings in primary human cells.
367 Therefore, we performed LPS stimulation experiments in magnetic-activated cell sorted (MACS)
368 $CD14^+$ monocytes from healthy volunteers and collected the cells at 6h, 12h and 18h after LPS
369 addition (Fig. 6 G&H, Fig. S8 A&B for 6h and 18h timepoints). To further challenge the cholinergic
370 link, we used nicotine as an immunosuppressive agent (Fig. S8C) (29). LPS-stimulated primary
371 $CD14^+$ cells presented significant upregulation of 4 out of the 6 stroke-induced tRFs at 12h, an
372 effect which was augmented by the addition of nicotine. Interestingly, at 18h, the tRF levels in the
373 LPS + nicotine group were comparable to those of nonstimulated cells (Fig. S8B). Together,
374 these findings demonstrate evolutionarily conserved and cholinergic-regulated increases of
375 stroke-induced tRFs under pro-inflammatory insults.
376
377 **Figure 6. tRF changes upon LPS stimulation of murine RAW 264.7 macrophages and**
378 **human $CD14^+$ monocytes and tRF-mimic transfection.** A) LPS stimulation of RAW 264.7
379 murine macrophage cells induced clear morphologic changes within 18h. Extracted RNA was
380 subjected to size selection and cDNA synthesized from the ≤50 nt fraction alone. Scale bar =
381 100µm. B) LPS-stimulated RAW 264.7 cells show dexamethasone-suppressible elevated levels
382 of post-stroke induced tRFs. Normalized RT-qPCR values (using mmu-miR-30d-5p, mmu-let7d-
383 5p as house-keeping transcripts, Supplementary Methods), compared to unstimulated controls.
384 Each dot represents 2-4 technical replicates, ANOVA with Tukey post-hoc, * $p < 0.05$, ** $p < 0.01$,
385 bar graphs +/- standard deviation (SD(lg)). C) Murine Zbp1 sequence carries an 8 nucleotides-
386 long fragment in the 3'UTR complementary to tRF-22-WE8SPOX52. D) To test the miR-like
387 mechanism of action, RAW 264.7 cells were transfected with ssRNA tRF-22-WE8SPOX mimics
388 or negative control ssRNA, and RNA was extracted 24h after transfection and subjected to polyA-
389 selected RNA sequencing (E) and RT-qPCR (F). E) Long RNA sequencing of cells transfected
390 with ssRNA tRF-22-WE8SPOX52 mimics revealed significantly downregulated expression of Z-
391 DNA binding protein (Zbp1) as compared to negative control (NC). * $p < 0.05$, shown is adjusted
392 p-value of Wald test via DESeq2, bar graph +/- SD. F) RT-qPCR from an independent cell culture
393 experiment confirmed the downregulation of Zbp1 expression after ssRNA tRF-22-WE8SPOX52
394 mimic transfection (relative normalized expression using Gapdh as a house-keeping gene), * $p <$
395 0.05 one-way ANOVA, each dot represents a technical cell culture replicate, bar graph +/-SD(lg)
396 G) MACS-sorted $CD14^+$ cells from healthy human donors were stimulated with LPS with or
397 without addition of nicotine and collected 6h, 12h and 18h thereafter. Extracted RNA was
398 subjected to size selection and cDNA synthesized from the ≤50 nt fraction. Timepoints 6h and
399 18h are shown in Figure S8. H) At 12h after LPS stimulation, human monocytes exhibited
400 upregulation of post-stroke induced tRFs as compared to unstimulated controls or cells treated
401 with nicotine alone. This reaction was boosted by the addition of nicotine. Shown is relative
402 expression (hsa-miR-30d and hsa-let7d-5p were used as house-keeping transcripts, see
403 Supplementary Methods) normalized to the nonstimulated group. Each dot represents one donor.
404 ANOVA with Tukey post-hoc, * $p < 0.05$, ** $p < 0.01$, *** $p < 0.001$ vs. non-stimulated cells; $^{\#} p <$
405 0.05, $^{\#\#} p < 0.01$, $^{\#\#\#} p < 0.001$ vs. cells upon addition of nicotine, bar graphs +/- SD(lg).

406

407 **Discussion**

408

medRxiv preprint doi: https://doi.org/10.1101/2020.07.02.20144212; this version posted October 7, 2020. The copyright holder for this preprint (which was not certified by peer review) is the author/funder, who has granted medRxiv a license to display the preprint in perpetuity.
It is made available under a CC-BY-NC-ND 4.0 International license .

409 To date, few studies have simultaneously assessed the joint impact of blood miR and tRF-
410 changes in human disease. Here we have discovered a stroke-induced decline of miRs and
411 concomitant elevation of tRFs in whole blood, and demonstrated that this shift may be associated
412 with the post-stroke cholinergic blockade of immune function. To validate our RNA-seq findings of
413 tRNA fragments in a way that circumvents the ambiguous detection of full-length tRNA, we
414 developed and used a size selection-based RT-qPCR test in an independent cohort of patients.
415 Mining transcriptomic datasets identified $CD14^+$ monocytes as likely pivotal in the cholinergic
416 control of immunity, demonstrated that the stroke-induced tRFs may target specific monocytic
417 TFs, and showed that at least some of those tRFs may actively control processes linked to
418 inflammatory responses. Moreover, several of the stroke-induced tRFs were also induced in LPS-
419 exposed murine macrophages and in human $CD14^+$ primary cells and showed time-dependent
420 nicotine- and dexamethasone-induced upregulation/suppression, supporting the notion that the
421 elevation of tRFs is an evolutionarily conserved response mechanism. Overexpression of tRF-22-
422 WE8SPOX52 using ssRNA mimics led to the downregulation of its Zbp1 target, which is involved
423 in regulating inflammatory responses. This concept of integrated fine-tuning of post-stroke
424 immune responses opens new venues for stroke diagnostics and therapeutics.
425
426 The cholinergic anti-inflammatory reflex plays a substantial role in regulating peripheral immune
427 responses after CNS injury, along with the HPA axis and sympathetic signaling (3). Excessive
428 cholinergic responses suppress pulmonary innate immunity, including macrophage and alveolar
429 epithelial cell responses; this may facilitate the development of pneumonia (30), a major factor of
430 non-recovery (31). However, while reduced AChE activities in post-stroke patients' serum
431 associate with poor survival (32), stroke-induced immunosuppression may be brain-protective (2),
432 calling for caution when considering therapeutic boosting of immune reaction in the periphery to
433 limit infections. Therefore, an in-depth understanding and characterization of the molecular
434 regulators of immune responses and the cholinergic pathway after CNS-injury is of utmost
435 importance at both the system and mechanism levels.
436
437 **System-level perturbations associated with ischemic stroke**.
438 We identified $CD14^+$ monocytes to be the most likely immune cell subpopulation for a
439 transcriptional cholinergic response. Monocytes play established roles in responses to stroke
440 including prolonged monocytosis, deactivation and functional impairment of circulating
441 monocytes/macrophages observed in experimental models (33) and human patients (34).
442 Moreover, stroke leads to overproduction of $CD14^{++}/CD16^-$ (classical) and $CD14^{++}/CD16^+$
443 (intermediate) monocytes with simultaneous decrease in $CD14^+/CD16^{++}$ (nonclassical)
444 monocytes, which correlates with stroke-associated infection (35). Relatedly, immune cells in
445 general, and monocytes in particular appear to be enriched in specific small RNA species
446 (compare Fig. 3C and (36)), and several of the most highly-perturbed small RNAs are abundantly
447 expressed in monocytes (compare Fig. S4, (37)).
448
449 Our in-depth analysis of the pathways targeted by perturbed miRs supports a tie between stroke-
450 induced changes and a cholinergic response. Both the identified clusters as well as the genes
451 enriched in each cluster may be further investigated for identifying the diverse mechanisms
452 involved. A recent whole blood microarray survey identified 15 miRs, 11 of which were replicated
453 in our study, to be suppressed within less than 72 hours in intracerebral hemorrhage patients
454 compared to controls (38). Those miRs pointed towards the same processes we found, including
455 inflammation and humoral immunity via JAK/STAT-activating cytokines, vascular integrity, and
456 the cellular immune response (38).
457
458 Stroke is a sudden incident with rapid onset and drastic systemic changes within a short time
459 frame. In the response to such immunologic emergencies, translational control is an important
460 tool (39) That tRFs may be rapidly produced by regulated nuclease cleavage of pre-existing
461 tRNAs in a "burst-like" fashion makes them particularly appropriate for handling acute situations.
462 Recent reports demonstrate production of 3'-tRFs by specific nucleases, and 3'- and 5'-tRNALeu

medRxiv preprint doi: https://doi.org/10.1101/2020.07.02.20144212; this version posted October 7, 2020. The copyright holder for this preprint (which was not certified by peer review) is the author/funder, who has granted medRxiv a license to display the preprint in perpetuity.
It is made available under a CC-BY-NC-ND 4.0 International license .

463 fragments were shown to regulate T cell activation (40). Furthermore, tRFs can perform different
464 molecular roles, including Ago-mediated suppression of target genes carrying complementary
465 sequence motifs (13). At least two of the stroke-induced tRFs upregulated after LPS stimulation
466 show miR-like function: tRF-22-WE8SPOX52 regulates B cell growth via suppressing the
467 expression of Replication Protein A1 (RPA1) (21) and a 17 nucleotides-long analog of tRF-18-
468 HR0VX6D2 limits cancer cell proliferation by impacting the cholinergic-regulating Notch signaling
469 pathway (22). Interestingly, hsa-miR-1260b, identified in our study and by others as perturbed
470 post-stroke (41) differs from tRF-18-HR0VX6D2 by only one nucleotide at position 9 and an
471 additional nucleotide at the 3'-end (Fig. S9), which indicates that hsa-miR-1260b may actually be
472 a tRF (42), and calls for further investigations.
473
474 Our study identified two main factors that may lead to an overall decrease in transcript regulation
475 by miRs after stroke. Firstly, the majority of miRs perturbed in our patient collective were
476 downregulated, and secondly, the downregulated miRs possessed significantly more targets than
477 the upregulated ones. For many processes regulated by these miRs, the resultant effect will
478 hence be de-repression of targeted genes (compare Fig. 5A). Additionally, we have identified a
479 stark dichotomy between the target sets of miRs and tRFs, indicating much complementarity and
480 only little cooperative overlap of affected transcripts between those two small RNA species (Fig.
481 5E). However, these changes may still lead to a homeostatic *functional* cooperation. In summary,
482 the post-stroke “changing of the guards” in the small RNA response may lead to preferential de-
483 repression of miR targets and concomitant repression of tRF targets, and the de-repression of
484 miR targets may be as pivotal for regulating the initial inflammatory response and subsequent
485 peripheral immunosuppression as the tRF elevation we identified.
486
487 Kinetically, stroke is characterized by an initial inflammatory response followed by
488 immunosuppression facilitated by, among others, the cholinergic anti-inflammatory reflex (3).
489 Therefore, the time-dependent elevation of tRFs and Cholino-tRFs in particular may offer new
490 mechanisms of homeostatic fine-tuning in response to cerebral ischemia. Further, not only the
491 peripheral but also the central immune response at the site of the injury is of great importance for
492 stroke prognosis. Brain injury triggers activation of microglia and infiltration of peripheral immune
493 cells, including monocyte-derived macrophages, which accumulate at the lesion site 3-7 days
494 after stroke (35). Experimental evidence highlights essential roles of these cells in CNS-repair
495 processes and neuronal protection (43, 44), and our own studies indicate small RNA-regulated
496 cross-talk between neuronal and immunological regulation by JAK/STAT-related mechanisms
497 (19).
498
499 Our current study presents tRFs as potential players in regulating the post-stroke inflammatory
500 responses. For example, KLF4, identified as down-regulated in our sequencing dataset, is
501 involved in controlling the macrophage response to LPS (28) and the differentiation of monocytes
502 towards an inflammatory phenotype (45). Therefore, a decrease in miRs targeting this TF may
503 contribute to pro-inflammatory monocytic response observed in the initial phase of stroke.
504 Similarly, MAFB is essential in facilitating the clearance of damage-associated molecular patterns
505 (DAMPs) in the ischemic brain, and, consequentially, limiting the inflammatory response while
506 supporting recovery (46). MAFB de-repression in peripheral immune cells may be a mechanism
507 supporting monocyte infiltration of the brain. Conversely, STAT1 and ATF3 may be preferentially
508 repressed due to their targeting by tRFs. STAT1 is essential in IFN- and IL-6-mediated
509 inflammatory response, and ATF3 is similarly induced by IFNs and contributes to STAT activity
510 via inhibition of STAT-dephosphorylating phosphatases (47, 48). Additionally, ATF3 down-
511 regulates AChE expression during stress (49). Whether these processes contribute to body
512 homeostasis after the damaging event, or rather to pathologic derailment of immune function,
513 requires detailed kinetic studies of circulating monocytes and brain-infiltrating monocyte-derived
514 macrophages, with simultaneous profiling of short and long transcripts.
515

516 **Mechanistic implications of tRF regulation after ischemic stroke**

medRxiv preprint doi: https://doi.org/10.1101/2020.07.02.20144212; this version posted October 7, 2020. The copyright holder for this preprint (which was not certified by peer review) is the author/funder, who has granted medRxiv a license to display the preprint in perpetuity.
It is made available under a CC-BY-NC-ND 4.0 International license .

517 To gain new insight into the regulation of inflammation by stroke-induced tRFs, we quantified the
518 top 6 perturbed tRFs in RAW 264.7 murine macrophages and primary LPS-stimulated $CD14^+$
519 human monocytes. Both cell types responded to LPS by upregulation of these tRFs within 12-
520 18h. Interestingly, dexamethasone prevented or subsequently downregulated the increased
521 expression of tRFs in the RAW 264.7 cells. To further seek cholinergic links of these stroke-
522 regulated tRFs, we used nicotine as an immunosuppressive stimulus in LPS-stimulated human
523 $CD14^+$ cells. Monocytes and macrophages express the cholinergic nicotinic alpha 7 receptor,
524 which after binding of acetylcholine downregulates the production of inflammatory cytokines (e.g.
525 TNFα) (29). In human $CD14^+$ cells, the levels of the top 6 stroke-induced tRFs were transiently
526 elevated by the addition of nicotine at the 12h timepoint (back to baseline by 18h post-
527 stimulation). Thus, the elevated levels of blood tRFs two days after ischemic stroke may reflect
528 potentiated cholinergic signaling, which remains to be investigated in the clinical setting.
529
530 In human patients, the stroke response in blood is cell type- and time-specific. For example, day
531 two post-ischemia features a transient increase in STAT3 phosphorylation of monocyte subsets,
532 which is also detected in patients after major surgery (50). Conversely, STAT3 signaling causes
533 immune stimulation in monocytes but is linked to immunosuppression in monocytic myeloid-
534 derived suppressor cells (M-MDSC) (50). Therefore, the biological activities of stroke-induced
535 tRFs are very likely also cell type- and context-specific. Our ssRNA tRF-22-WE8SPOX52 mimic
536 experiments further support tRF involvement in the posttranscriptional regulation of genes
537 implicated in inflammatory responses. Zbp1, which was significantly downregulated under tRF-
538 22-WE8SPOX52 overexpression, is a DAMP-sensor which induces interferon responses,
539 programmed cell death, and NLRP3 inflammasome formation (51). The ZBP1 protein has often
540 been linked to the response to viral infections, but some studies point to its role in the reaction to
541 bacterial pathogens, where it may be involved in the induction of necroptosis (51). Incidentally,
542 the ZBP1 transcript is also downregulated in our long RNA sequencing of patient blood (logFC = -
543 1.7, adjusted p-value = 0.001); the exact nature of the interaction of tRF-22-WE8SPOX52 and
544 ZBP1 should be subject of future studies.
545
546 **Limitations**
547 We hypothesized that the tRFs identified in our study are of cellular origin and therefore re-
548 analyzed the small RNA sequencing data provided by Juzenas et al. (GSE100467). While some
549 studies identified an enrichment of tRFs in exosomes (40), our re-analysis found the tRFs mostly
550 in the cellular blood compartments. Although the main immune populations are included in the
551 analyzed dataset, it should be noted that the tRFs identified in our study may also originate from
552 immune cells not sorted/sequenced by Juzenas et al. Additionally, considering the different roles
553 of specific immune subpopulations, identifying the specific source of tRFs and their roles in
554 immune function should be the goal of further investigations. For example, monocyte subsets are
555 differentially regulated after stroke, and since these cells all express the CD14 marker (35), a
556 higher cellular resolution is called for. Also, tRFs are induced upon cellular stress (52), such that
557 the sorting procedure may affect their expression, and they may reside in extracellular
558 compartments (15, 53), calling for testing the impact of sample processing, RNA isolation and
559 sequencing techniques on the detectability of tRFs. Additionally, a method for the direct
560 comparison of miR- and tRF-levels in the same sequencing experiment will be important for
561 discerning the true difference in detected counts after alignment, possibly via spike-in procedures.
562 The currently maturing technology of single-cell sequencing is an obvious candidate for achieving
563 the goals of higher cellular resolution along with avoiding stressors associated with sample
564 preparation, but its shallow sequencing depth is still an issue.
565
566 Given the sex-related differences in cholinergic responses (54), the molecular regulators of
567 cholinergic signaling and immunity should be investigated in detail in both males and females.
568 However, to increase the consistency of our results, we only included male stroke patients, which
569 is a further limitation of this study. Interestingly, the overall impact of stroke is greater in women,
570 as their higher life expectancy is linked to increased stroke incidence in older adults, and they

medRxiv preprint doi: https://doi.org/10.1101/2020.07.02.20144212; this version posted October 7, 2020. The copyright holder for this preprint (which was not certified by peer review) is the author/funder, who has granted medRxiv a license to display the preprint in perpetuity.
It is made available under a CC-BY-NC-ND 4.0 International license .

571 face worse recovery prospects (55). Last, but not least, tRFs may have functions other than their
572 miR-like activities; for instance, tRNALeu-CAG fragments facilitate translation and ribosome
573 biogenesis (12), whereas tRNAGly, tRNAGlu, tRNAAsp and tRNATyr-derived tRFs displace
574 RNA-binding proteins leading to mRNA destabilization (11). Therefore, potential functions of
575 stroke-perturbed tRFs other than Ago-mediated suppression of translation should be further
576 examined.
577

578 **Conclusion**

579 While the specific roles of tRFs in regulating local neuroinflammatory responses and functional
580 modulation of specific peripheral monocyte subsets remain to be elucidated, our findings point
581 towards tRFs/miRs as homeostatic regulators of post-stroke immune responses and potential
582 biomarkers for increased infection risk in these patients. The cumulative role of tRFs and miRs as
583 general post-damage mediators of CNS-immune communication thus calls for seeking small
584 RNAs, and tRFs in particular, as involved in other traumatic pathologies such as spinal cord
585 injury, traumatic brain injury, concussion, as well as neuroinflammatory brain diseases.
586
587

588 ## Materials and Methods

589
590 Expanded methods can be found in the online supplement.
591

592 ### Clinical cohort

593 PREDICT was a prospective multi-center study with sites in Germany and Spain
594 (www.clinicaltrials.gov, NCT01079728)(16) that analyzed 484 acute ischemic stroke patients.
595 Patients underwent daily screenings for stroke-associated pneumonia, dysphagia and
596 inflammation markers and their clinical outcome was recorded 3 months post-stroke. To exclude
597 very severe cases of stroke, we only considered for sequencing samples from patients with
598 modified Rankin Scale (mRS) values of 3 and below at discharge from the hospital, leaving
599 n=240 relevant cases. Blood was collected into RNA stabilizing tubes (Tempus Blood RNA tubes,
600 Applied Biosystems^{TM}) on each day of hospitalization. Blood samples collected on the 2nd day
601 were subjected to small and long RNA-sequencing, with time from stroke occurrence to blood
602 withdrawal varying between 0.94 to 2.63 days (average: 1.98 days). Blood samples from age-
603 and ethnicity-matched healthy controls were obtained at matched circadian time from donors with
604 ethical approvals from institutional review boards (ZenBio, North Carolina, USA).
605

606 ### RNA extraction, quality control and sequencing

607 RNA was extracted from 3 ml of whole blood of 484 PREDICT patients using Tempus Spin RNA
608 isolation kit (Invitrogen, Thermo Fisher Scientific, Waltham MA, USA). Pre-sequencing
609 Bioanalyzer 6000 (Agilent, Santa Clara CA, USA) tests showed high RNA quality (RIN values 7.9-
610 9.9, median 8.8). Libraries constructed from 600 ng total RNA of 43 samples were subjected to
611 small RNA-sequencing (NEBNext® Multiplex Small RNA library prep set for Illumina, New
612 England Biolabs, Ipswich MA, USA), and 24 of the small RNA-sequenced samples served for
613 PolyA-selected long mRNA sequencing (1000 ng total RNA per sample, TruSeq RNA library
614 preparation kit (Illumina, San Diego CA, USA)). Sequencing (24 or 12 samples per flow cell for
615 small and long RNAs, respectively) was performed on the Illumina NextSeq 500 platform at the
616 Hebrew University's Center for Genomic Technologies.
617

618 ### Alignment and count table generation of RNA sequencing reads

619 Quality control was performed using FastQC, version 0.11.2 (56) more details can be found in the
620 Supplementary Methods. Flexbar (with parameters "-q TAIL -qf Sanger -qw 4 -min-read-length
621 16") (57) served for adapter trimming and quality based filtering of all raw reads. Long RNA was
622 aligned to the human reference transcriptome (ENSEMBL GRCh38 release 79) using salmon
623 (58) with default parameters. Small RNA was aligned to the miRBase version 21 using
624 miRExpress 2.1.4 (59) with default parameters but skipping adapter trimming for miR expression,

medRxiv preprint doi: https://doi.org/10.1101/2020.07.02.20144212; this version posted October 7, 2020. The copyright holder for this preprint (which was not certified by peer review) is the author/funder, who has granted medRxiv a license to display the preprint in perpetuity.
It is made available under a CC-BY-NC-ND 4.0 International license .

625 and to the tRNA transcriptome using the MINTmap pipeline (60) with default parameters for tRF
626 expression (using only reads mapping exclusively to the tRNA space). Raw gene-expression
627 data of small and long RNA sequencing and technical covariates of all experiments are available
628 via the NCBI GEO database (accession number GSE158312).
629
630 **Size selection for tRF quantification**
631 Standard RT-qPCR methods do not allow to distinguish between full length tRNA molecules and
632 3'tRFs. To exclude longer RNA species in the RT-qPCR quantifications, we performed RNA size
633 selection on 15% TBE-Urea-Polyacrylamide gels, selecting only RNA molecules ≤ 25 nucleotides
634 for validations in the clinical cohort and ≤ 50 nucleotides for the assessment of tRF expression in
635 LPS-stimulated RAW 264.7 cells and human CD14$^+$ monocytes. Detailed description can be
636 found in the Supplementary Methods.
637
638 **Analysis of the presence/absence of specific tRFs in blood compartments**
639 In descriptive analysis of small RNA expression, a threshold (e.g., at least 5 counts in at least
640 80% of samples) is often used to define presence or absence of small RNAs. However, since this
641 definition relies heavily on sequencing depth, and depth can vary widely even in methodically
642 robust sequencing experiments depending on a large number of variables, we defined our own
643 test for descriptive analysis of presence or absence of lowly expressed small RNAs in each of the
644 sample types. Briefly, this definition comprises estimation of a log-normal distribution on the
645 expression profile of the small RNA across all samples in the individual cell types, and a statistical
646 test to refute the null hypothesis that the distribution is in fact log-normal. For each small RNA,
647 the distribution mean and standard deviation of the expression values per cell type were
648 estimated using the *fitdist* function of the R/fitdistrplus package (61). The count distribution was
649 then tested against a log-normal distribution with the estimated mean and standard deviation via
650 the R implementation of the Kolmogorov-Smirnov test, with a cutoff of 0.1. The small RNA was
651 defined as present if the test failed to reject the null hypothesis (see Fig. S4 for examples). The
652 code implementation is available at https://github.com/slobentanzer/stroke-trf.
653
654 **LPS stimulation of murine macrophages**
655 Murine RAW 264.7 cells (ATCC TIB-71) cultured in Dulbecco's Modified Eagle's Medium
656 supplemented with 10% Fetal Calf Serum, 1% Penicillin-Streptomycin-Amphotericin B and 1% L-
657 Glutamine (all reagents from Biological Industries, Beit HaEmek, Israel) were collected using a
658 cell scraper and stimulated with lipopolysaccharide (LPS from *E.coli* 0127:B8, Sigma Aldrich, St.
659 Louis, USA) following modified protocol (62). Briefly, 2e05 cells were stimulated with 100 ng/ml
660 LPS +/- 0.5 µM dexamethasone per well (Sigma Aldrich, St. Louis, USA) in 12-well cell culture
661 plates. Cells were collected in Tri-Reagent (Sigma Aldrich, St. Louis, USA) 18h after LPS
662 stimulation and RNA was isolated using miRNeasy kit (Qiagen, Hilden, Germany). For the size
663 selection, 1 µg of total RNA was used and cDNA was synthesized from 500 pg of size-selected
664 RNA using qScript microRNA cDNA Synthesis Kit (Quanta Biosciences, Beverly MA, USA) and
665 following standard protocol (for further details see Supplementary Methods). Data presented in
666 the manuscript is derived from 3 independent experiments (2 of them with dexamethasone
667 treatment) with 2-4 technical replicates in each group.
668
669 **Transfection experiments with tRF-22-WE8SPOX52 mimics, RNA sequencing and RT-**
670 **qPCR**
671 Transfections were performed using HiPerFect transfection agent (Qiagen, Hilden, Germany)
672 following a standard protocol for transfecting RAW 264.7 macrophages. Briefly, 2e05 RAW 264.7
673 cells per well were seeded in 24-well plates and transfected using 6 µl HiPerFect reagent per well
674 and 50 nM final ssRNA tRF-mimics: /5PHOS/rArU rCrCrC rArCrC rGrCrU rGrCrC rAmCmC rA,
675 using NC5 /5PHOS/rGrC rGrArC rUrArU rArCrG rCrGrC rArArU mAmUrG (both from IDT,
676 Coralville IA, USA) as negative control. Cells were collected after 24h following the transfection in
677 Tri-Reagent (Sigma Aldrich, St. Louis, USA) and total RNA isolated using the miRNeasy kit
678 (Qiagen, Hilden, Germany). Two separate experiments were performed: [1] 180 ng RNA was

medRxiv preprint doi: https://doi.org/10.1101/2020.07.02.20144212; this version posted October 7, 2020. The copyright holder for this preprint (which was not certified by peer review) is the author/funder, who has granted medRxiv a license to display the preprint in perpetuity.
It is made available under a CC-BY-NC-ND 4.0 International license .

679 subjected to long RNA sequencing (KAPA stranded mRNA-seq kit, Roche, Basel Switzerland)
680 and [2] Zbp1 levels were quantified by RT-qPCR (relative expression normalized to Gapdh) after
681 cDNA synthesis (qScript Kit; Quanta Biosciences, Beverly MA, USA) from 100 ng RNA.
682

683 **Isolation and *ex vivo* stimulation of human monocytes**

684 This study was approved by the ethics committees of the Charité Universitätsmedizin Berlin (MG
685 Cohort: EA1/281/10). Peripheral blood mononuclear cells (PBMCs) were separated from whole
686 blood anticoagulated with heparin by density gradient centrifugation over Ficoll (Biocoll separating
687 solution, Biochrom GmbH, Berlin, Germany). Untouched monocytes were isolated by using a
688 commercially available Pan Monocyte Isolation Kit (Miltenyi Biotec, Bergisch Gladbach,
689 Germany). Cells (2e06 cells/ml) were cultured in RPMI 1640 Medium (VWR, Radnor, USA),
690 supplemented with 1% penicillin-streptomycin (Biochrom GmbH, Berlin, Germany), 2mM L-
691 Glutamine (Biochrom GmbH, Berlin, Germany) and 10% autologous serum and stimulated with
692 LPS (1ng/ml, 0127:B8, Sigma, Kawasaki, Japan) in the presence or absence of nicotine (300μM,
693 Sigma, Kawasaki, Japan) for 6h, 12h and 18h at 37°C. Unstimulated monocytes and monocytes
694 stimulated with nicotine served as controls. Tumor necrosis factor α (TNFα) concentration was
695 measured in cell culture supernatant by using a commercially available DuoSet ELISA kit (R&D
696 systems, Minneapolis, USA). Cells were collected in Tri-Reagent (Sigma Aldrich, St. Louis, USA)
697 and RNA was isolated using miRNeasy kit (Qiagen, Hilden, Germany). For the size selection, 600
698 ng of total RNA (or maximum loading volume of 20 μl) were used and cDNA was synthesized
699 from 500 pg of size-selected RNA using qScript microRNA cDNA Synthesis Kit (Quanta
700 Biosciences, Beverly MA, USA) and following standard protocol (for further details see
701 Supplementary Methods).
702
703

704 **Statistical analysis**

705 Data analysis was performed using R (version 4.0.2), the code is available at
706 https://github.com/slobentanzer/stroke-trf (including code for analyses of RT-qPCR data) FDR
707 correction was applied whenever applicable. RT-qPCR data was analyzed using Bio-Rad CFX
708 Maestro software (Bio-Rad, Version 4.1.2433.1219) and plotted in GraphPad Prism 8.0
709 (GraphPad Prism Software Inc., San Diego, USA).
710
711

712 **Acknowledgments**

713
714 The authors would like to thank Dr. Simonas Juzenas (Saarbrücken) and Prof. Andreas Keller
715 (Saarbrücken/Stanford) for their support concerning the blood compartments RNA-sequencing
716 dataset and Dr. Iftach Shaked (San Diego) for fruitful discussions.
717
718

719 **Funding**

720 This study was supported by the European Research Council Advanced Award 321501, the
721 Israel Science Foundation grant 1016/18, the Israeli Ministry of Science, Technology and Space
722 Grant No. 53140 (to H.S), as well as by the German Research Foundation (Exc257, TR84,
723 SFB/TRR167) (to A.M and C.M), the Leducq Foundation (19CVD01) and the Einstein
724 Foundation, Berlin (A-2017-406 to A.M and H.S). Further support was provided by a NeuroCure
725 visiting fellowship (to H.S), as well as by Edmond and Lily Safra Center of Brain Science (ELSC)
726 post-doctoral fellowships to S.S-T and K.W. K.W is a Shimon Peres Post-doctoral Fellow at the
727 ELSC and S.L received an ELSC fellowship for visiting PhD students.
728
729

730 **References**

731
732 1. C. O. Johnson, *et al.*, Global, regional, and national burden of stroke, 1990–2016: a

medRxiv preprint doi: https://doi.org/10.1101/2020.07.02.20144212; this version posted October 7, 2020. The copyright holder for this preprint (which was not certified by peer review) is the author/funder, who has granted medRxiv a license to display the preprint in perpetuity.
It is made available under a CC-BY-NC-ND 4.0 International license .

733 systematic analysis for the Global Burden of Disease Study 2016. *Lancet Neurol.* **18**, 439–
734 458 (2019).
735 2. U. Dirnagl, *et al.*, Stroke-induced immunodepression: experimental evidence and clinical
736 relevance. *Stroke* **38**, 770–773 (2007).
737 3. C. Meisel, J. M. Schwab, K. Prass, A. Meisel, U. Dirnagl, Central nervous system injury-
738 induced immune deficiency syndrome. *Nat Rev Neurosci* **6**, 775–786 (2005).
739 4. M. Rosas-Ballina, *et al.*, Acetylcholine-synthesizing T cells relay neural signals in a vagus
740 nerve circuit. *Science (80-.).* **334**, 98–101 (2011).
741 5. L. V. Borovikova, *et al.*, Vagus nerve stimulation attenuates the systemic inflammatory
742 response to endotoxin. *Nature* **405**, 458–462 (2000).
743 6. I. Shaked, *et al.*, MicroRNA-132 potentiates cholinergic anti-inflammatory signaling by
744 targeting acetylcholinesterase. *Immunity* **31**, 965–973 (2009).
745 7. H. Soreq, Checks and balances on cholinergic signaling in brain and body function.
746 *Trends Neurosci* **38**, 448–458 (2015).
747 8. A. G. Torres, O. Reina, C. Stephan-Otto Attolini, L. Ribas de Pouplana, Differential
748 expression of human tRNA genes drives the abundance of tRNA-derived fragments. *Proc.*
749 *Natl. Acad. Sci. U. S. A.* **116**, 8451–8456 (2019).
750 9. S. Yamasaki, P. Ivanov, G. F. Hu, P. Anderson, Angiogenin cleaves tRNA and promotes
751 stress-induced translational repression. *J Cell Biol* **185**, 35–42 (2009).
752 10. L. Huang, H. Guo, M. Cheng, Y. Zhao, X. Jin, The kinetic change of the serum angiogenin
753 level in patients with acute cerebral infarction. *Eur. Neurol.* **58**, 224–227 (2007).
754 11. H. Goodarzi, *et al.*, Endogenous tRNA-Derived Fragments Suppress Breast Cancer
755 Progression via YBX1 Displacement. *Cell* **161**, 790–802 (2015).
756 12. H. K. Kim, *et al.*, A transfer-RNA-derived small RNA regulates ribosome biogenesis.
757 *Nature* **552**, 57 (2017).
758 13. P. Kumar, J. Anaya, S. B. Mudunuri, A. Dutta, Meta-analysis of tRNA derived RNA
759 fragments reveals that they are evolutionarily conserved and associate with AGO proteins
760 to recognize specific RNA targets. *BMC Biol* **12**, 78 (2014).
761 14. Q. Li, *et al.*, TRNA-Derived Small Non-Coding RNAs in Response to Ischemia Inhibit
762 Angiogenesis. *Sci. Rep.* **6**, 20850 (2016).
763 15. M. C. Hogg, *et al.*, Elevation of plasma tRNA fragments precedes seizures in human
764 epilepsy. *J. Clin. Invest.* **129**, 2946–2951 (2019).
765 16. S. Hoffmann, *et al.*, Stroke-induced immunodepression and dysphagia independently
766 predict stroke-associated pneumonia - The PREDICT study. *J Cereb Blood Flow Metab*
767 **37**, 3671–3682 (2017).
768 17. P. Li, *et al.*, Identification of circulating microRNAs as potential biomarkers for detecting
769 acute ischemic stroke. *Cell Mol Neurobiol* **35**, 433–447 (2015).
770 18. G. C. Jickling, *et al.*, microRNA Expression in Peripheral Blood Cells following Acute
771 Ischemic Stroke and Their Predicted Gene Targets. *PLoS One* **9** (2014).
772 19. S. Lobentanzer, G. Hanin, J. Klein, H. Soreq, Integrative Transcriptomics Reveals
773 Sexually Dimorphic Control of the Cholinergic/Neurokine Interface in Schizophrenia and
774 Bipolar Disorder. *Cell Rep.* **29**, 764-777.e5 (2019).
775 20. V. Agarwal, G. W. Bell, J. W. Nam, D. P. Bartel, Predicting effective microRNA target sites
776 in mammalian mRNAs. *Elife* **4** (2015).
777 21. R. L. Maute, *et al.*, tRNA-derived microRNA modulates proliferation and the DNA damage
778 response and is down-regulated in B cell lymphoma. *Proc. Natl. Acad. Sci. U. S. A.* **110**,
779 1404–9 (2013).
780 22. B. Huang, *et al.*, Molecular and Cellular Pathobiology tRF/miR-1280 Suppresses Stem
781 Cell-like Cells and Metastasis in Colorectal Cancer (2017) https:/doi.org/10.1158/0008-
782 5472.CAN-16-3146 (January 30, 2019).
783 23. M. I. Love, W. Huber, S. Anders, Moderated estimation of fold change and dispersion for
784 RNA-seq data with DESeq2. *Genome Biol.* **15** (2014).
785 24. S. Juzenas, *et al.*, A comprehensive, cell specific microRNA catalogue of human
786 peripheral blood. *Nucleic Acids Res.* **45**, 9290–9301 (2017).

medRxiv preprint doi: https://doi.org/10.1101/2020.07.02.20144212; this version posted October 7, 2020. The copyright holder for this preprint (which was not certified by peer review) is the author/funder, who has granted medRxiv a license to display the preprint in perpetuity.
It is made available under a CC-BY-NC-ND 4.0 International license .

787 25. D. Marbach, *et al.*, Tissue-specific regulatory circuits reveal variable modular perturbations
788 across complex diseases. *Nat. Methods* **13**, 366–370 (2016).
789 26. D. W. Huang, B. T. Sherman, R. A. Lempicki, Systematic and integrative analysis of large
790 gene lists using DAVID bioinformatics resources. *Nat. Protoc.* **4**, 44–57 (2009).
791 27. K. Shuai, *et al.*, Interferon activation of the transcription factor Stat91 involves dimerization
792 through SH2-phosphotyrosyl peptide interactions. *Cell* **76**, 821–828 (1994).
793 28. M. W. Feinberg, *et al.*, Kruppel-like factor 4 is a mediator of proinflammatory signaling in
794 macrophages. *J. Biol. Chem.* **280**, 38247–38258 (2005).
795 29. T. Fujii, *et al.*, Expression and function of the cholinergic system in immune cells (2017).
796 30. O. Engel, *et al.*, Cholinergic Pathway Suppresses Pulmonary Innate Immunity Facilitating
797 Pneumonia after Stroke. *Stroke* **46**, 3232–3240 (2015).
798 31. O. Finlayson, *et al.*, Risk factors, inpatient care, and outcomes of pneumonia after
799 ischemic stroke. *Neurology* **77**, 1338–1345 (2011).
800 32. E. Ben Assayag, *et al.*, Serum cholinesterase activities distinguish between stroke
801 patients and controls and predict 12-month mortality. *Mol Med* **16**, 278–286 (2010).
802 33. L. McCulloch, A. Alfieri, B. W. McColl, Experimental stroke differentially affects discrete
803 subpopulations of splenic macrophages. *Front. Immunol.* **9**, 1108 (2018).
804 34. X. Urra, *et al.*, Monocyte subtypes predict clinical course and prognosis in human stroke.
805 *J. Cereb. Blood Flow Metab.* **29**, 994–1002 (2009).
806 35. A. ElAli, N. J. LeBlanc, The role of monocytes in ischemic stroke pathobiology: New
807 avenues to explore. *Front. Aging Neurosci.* **8** (2016).
808 36. P. Leidinger, C. Backes, B. Meder, E. Meese, A. Keller, The human miRNA repertoire of
809 different blood compounds. *BMC Genomics* **15** (2014).
810 37. S. Lobentanzer, "Small RNA Dynamics in Cholinergic Systems. Doctoral Dissertation,"
811 Goethe-University, Frankfurt, Germany. (2020).
812 38. X. Cheng, *et al.*, MicroRNA and their target mRNAs change expression in whole blood of
813 patients after intracerebral hemorrhage. *J. Cereb. Blood Flow Metab.*, 0271678X1983950
814 (2019).
815 39. C. A. Piccirillo, E. Bjur, I. Topisirovic, N. Sonenberg, O. Larsson, Translational control of
816 immune responses: from transcripts to translatomes. *Nat. Immunol.* **15**, 503–511 (2014).
817 40. N.-T. Chiou, R. Kageyama, K. M. Ansel, Selective Export into Extracellular Vesicles and
818 Function of tRNA Fragments during T Cell Activation. *Cell Rep.* **25**, 3356-3370.e4 (2018).
819 41. J. R. Tan, *et al.*, Blood microRNAs in low or no risk ischemic stroke patients. *Int. J. Mol.*
820 *Sci.* **14**, 2072–84 (2013).
821 42. N. C. T. Schopman, S. Heynen, J. Haasnoot, B. Berkhout, A miRNA-tRNA mix-up: tRNA
822 origin of proposed miRNA. *RNA Biol.* **7**, 573–576 (2010).
823 43. S. Wattananit, *et al.*, Monocyte-derived macrophages contribute to spontaneous long-term
824 functional recovery after stroke in mice. *J. Neurosci.* **36**, 4182–4195 (2016).
825 44. C. Cserép, *et al.*, Microglia monitor and protect neuronal function through specialized
826 somatic purinergic junctions. *Science (80-.).* **367**, 528–537 (2020).
827 45. M. W. Feinberg, *et al.*, The Kruppel-like factor KLF4 is a critical regulator of monocyte
828 differentiation. *EMBO J.* **26**, 4138–4148 (2007).
829 46. T. Shichita, *et al.*, MAFB prevents excess inflammation after ischemic stroke by
830 accelerating clearance of damage signals through MSR1. *Nat. Med.* **23**, 723–732 (2017).
831 47. L. I. Labzin, *et al.*, ATF3 Is a Key Regulator of Macrophage IFN Responses. *J. Immunol.*
832 **195**, 4446–4455 (2015).
833 48. D. Glal, *et al.*, ATF3 Sustains IL-22-Induced STAT3 Phosphorylation to Maintain Mucosal
834 Immunity Through Inhibiting Phosphatases. *Front. Immunol.* **9** (2018).
835 49. R. Heinrich, *et al.*, ATF3 Regulates the Expression of AChE During Stress. *Front. Mol.*
836 *Neurosci.* **11** (2018).
837 50. A. S. Tsai, *et al.*, A year-long immune profile of the systemic response in acute stroke
838 survivors. *Brain* **142**, 978–991 (2019).
839 51. T. Kuriakose, T. D. Kanneganti, ZBP1: Innate Sensor Regulating Cell Death and
840 Inflammation. *Trends Immunol.* **39**, 123–134 (2018).

medRxiv preprint doi: https://doi.org/10.1101/2020.07.02.20144212; this version posted October 7, 2020. The copyright holder for this preprint (which was not certified by peer review) is the author/funder, who has granted medRxiv a license to display the preprint in perpetuity.
It is made available under a CC-BY-NC-ND 4.0 International license .

841 52. D. M. Thompson, R. Parker, Stressing out over tRNA cleavage. *Cell* **138**, 215–219 (2009).
842 53. P. M. Godoy, *et al.*, Large Differences in Small RNA Composition Between Human
843 Biofluids. *Cell Rep.* **25**, 1346–1358 (2018).
844 54. S. Shenhar-Tsarfaty, *et al.*, Weakened cholinergic blockade of inflammation associates
845 with diabetes-related depression. *Mol. Med.* **22**, 156–161 (2016).
846 55. M. J. Reeves, *et al.*, Sex differences in stroke: epidemiology, clinical presentation, medical
847 care, and outcomes. *Lancet Neurol.* **7**, 915–926 (2008).
848 56. S. Andrews, FastQC: a quality control tool for high throughput sequence data. (2010).
849 57. Flexbar 3.0 – SIMD and multicore parallelization | Bioinformatics | Oxford Academic
850 (March 13, 2020).
851 58. R. Patro, G. Duggal, M. I. Love, R. A. Irizarry, C. Kingsford, Salmon provides fast and
852 bias-aware quantification of transcript expression. *Nat. Methods* **14**, 417–419 (2017).
853 59. W. C. Wang, *et al.*, miRExpress: analyzing high-throughput sequencing data for profiling
854 microRNA expression. *BMC Bioinformatics* **10**, 328 (2009).
855 60. P. Loher, A. G. Telonis, I. Rigoutsos, MINTmap: Fast and exhaustive profiling of nuclear
856 and mitochondrial tRNA fragments from short RNA-seq data. *Sci. Rep.* (2017)
857 https:/doi.org/10.1038/srep41184.
858 61. M. L. Delignette-Muller, C. Dutang, fitdistrplus: An R package for fitting distributions. *J.*
859 *Stat. Softw.* **64**, 1–34 (2015).
860 62. T. Bartosh, J. Ylostalo, Macrophage Inflammatory Assay. *BIO-PROTOCOL* **4** (2014).
861
862

863

A
Ischemic stroke
n = 33/484
Control
n = 10/20
RNA seq
miRs
tRFs

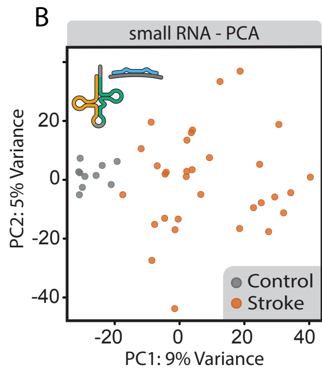
B
small RNA - PCA
PC2: 5% Variance
PC1: 9% Variance
Control
Stroke

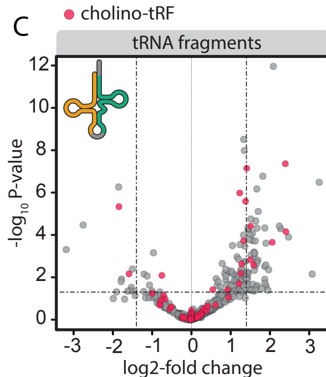
cholino-tRF
C
tRNA fragments
$-\log_{10}$ P-value
log2-fold change

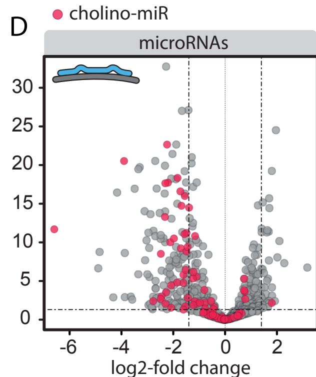
cholino-miR
D
microRNAs
log2-fold change

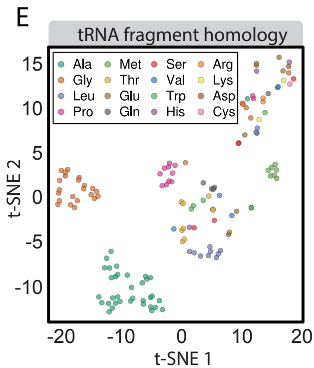
E
tRNA fragment homology
Ala
Met
Ser
Arg
Gly
Thr
Val
Lys
Leu
Glu
Trp
Asp
Pro
Gln
His
Cys
t-SNE 2
t-SNE 1

A

control stroke

normalized counts

6000 4000 2000 0

*** *** *** ** ** ***

RNA seq

tRF-22-WEKSPM852 tRF-18-8R6546D2 tRF-18-HR0VX6D2 tRF-18-8R6Q46D2 tRF-22-8EKSP1852 tRF-22-WE8SPOX52

B

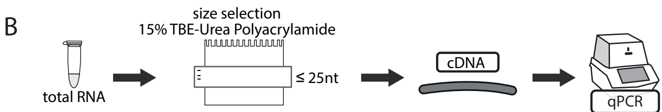

C

relative expression

5 4 3 2 1 0

*** *** *** *** *** **

tRF-22-WEKSPM852 tRF-18-8R6546D2 tRF-18-HR0VX6D2 tRF-18-8R6Q46D2 tRF-22-8EKSP1852 tRF-22-WE8SPOX52

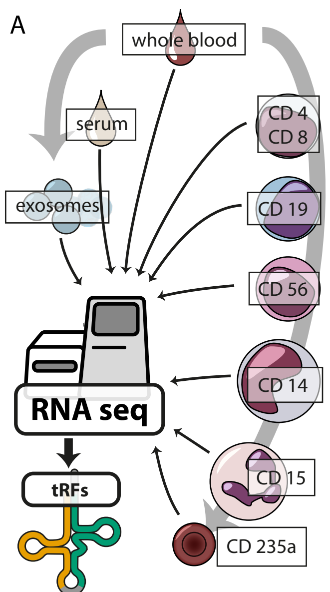
A
whole blood
serum
exosomes
CD 4
CD 8
CD 19
CD 56
CD 14
CD 15
CD 235a
RNA seq
tRFs

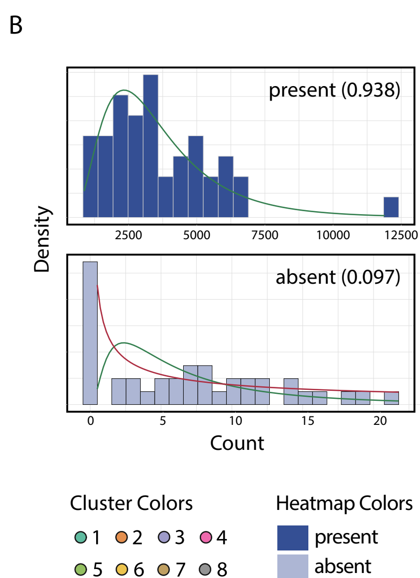
B
present (0.938)
absent (0.097)
Density
Count
Cluster Colors
1 2 3 4
5 6 7 8
Heatmap Colors
present
absent

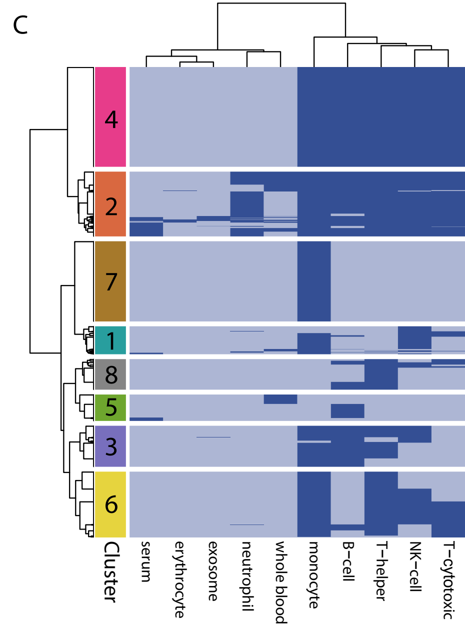
C
Cluster
serum
erythrocyte
exosome
neutrophil
whole blood
monocyte
B−cell
T−helper
NK−cell
T−cytotoxic

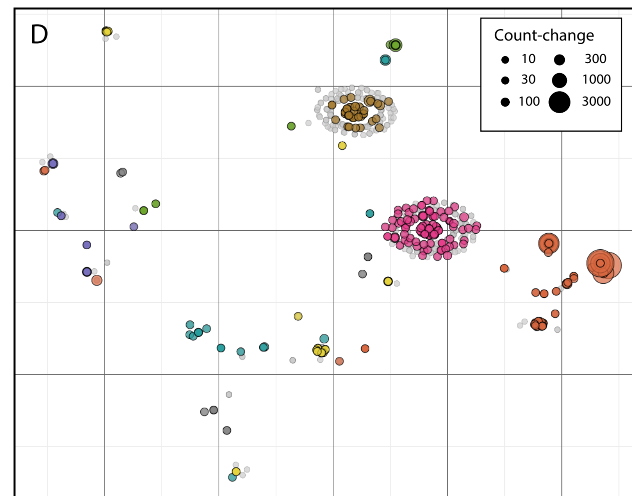
D
Count-change
10
30
100
300
1000
3000

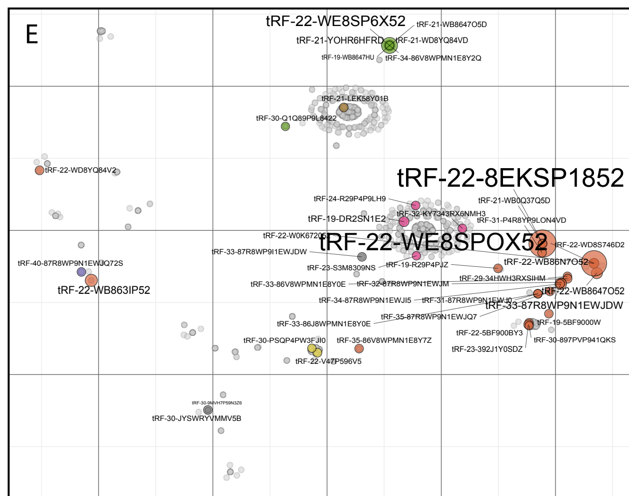
E
tRF-22-WE8SP6X52
tRF-22-8EKSP1852
tRF-22-WE8SPOX52
tRF-22-WB863IP52
tRF-33-87R8WP9N1EWJDW
tRF-22-WD8YQ84V2
tRF-21-LEK58Y01B
tRF-30-Q1Q89P9L8422
tRF-30-JYSWRYVMMV5B

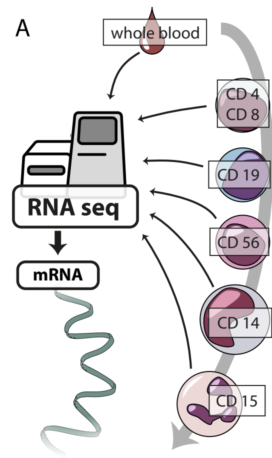

B
CHRM2
SLC18A3
ACHE
CHRNB1
CHRM1
COLQ
CHRNA6
CHRNA7
CHRNA2
CHRNE
CHRNA3
CHRNA5
CHRNA9
Cell Cluster
CD14POS_MONOCYTES
CD19POS_B_CELLS
CD4POS_T_CELLS
CD8POS_T_CELLS
NATURAL_KILLER_CELLS
NEUTROPHILS

C
cell-cell signaling
cell maturation
heterotypic cell-cell adhesion
homotypic cell-cell adhesion
negative regulation of T cell proliferation
platelet degranulation
localization within membrane
response to lipopolysaccharide
platelet activation
STAT cascade
regulation of interferon-gamma production
response to bacterium
positive regulation of smooth muscle cel...
negative regulation of angiogenesis
substrate adhesion-dependent cell spreading
cellular response to chemical stimulus
innate immune response
response to organophosphorus
response to purine-containing compound
positive regulation of cytokine production
negative regulation of cytokine production
regulation of type I interferon production
positive regulation of response to cytokine
response to exogenous dsRNA
cellular response to virus
cytoplasmic pattern recognition receptor signalling pathway
51
27
11
2

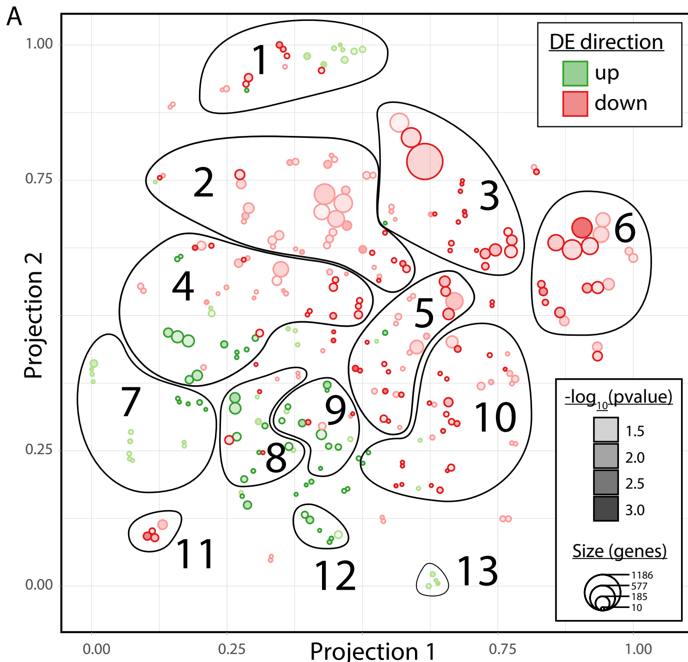

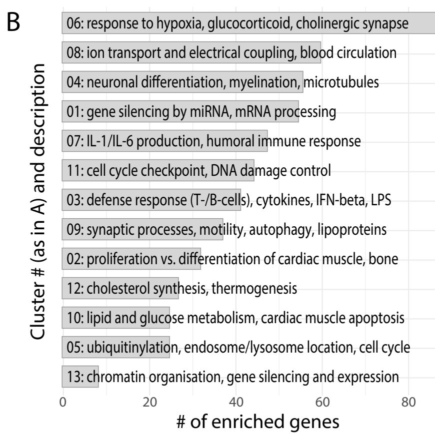

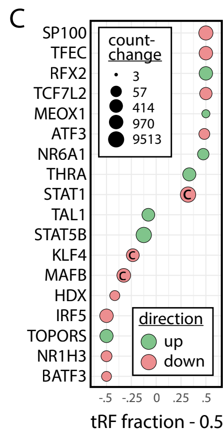

D
tRFs
miRs
TFs

E
RFX2
ATF3
SP100
STAT1
THRA
TFEC
STAT5B
MAFB
HDX
KLF4

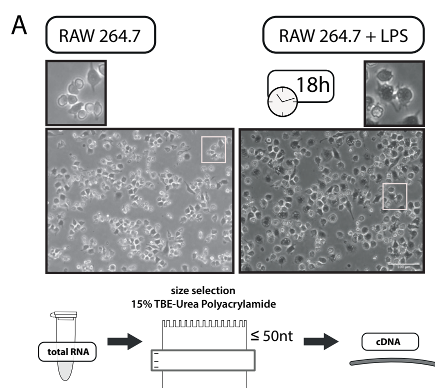
A
RAW 264.7
RAW 264.7 + LPS
18h
size selection
15% TBE-Urea Polyacrylamide
total RNA
≤ 50nt
cDNA

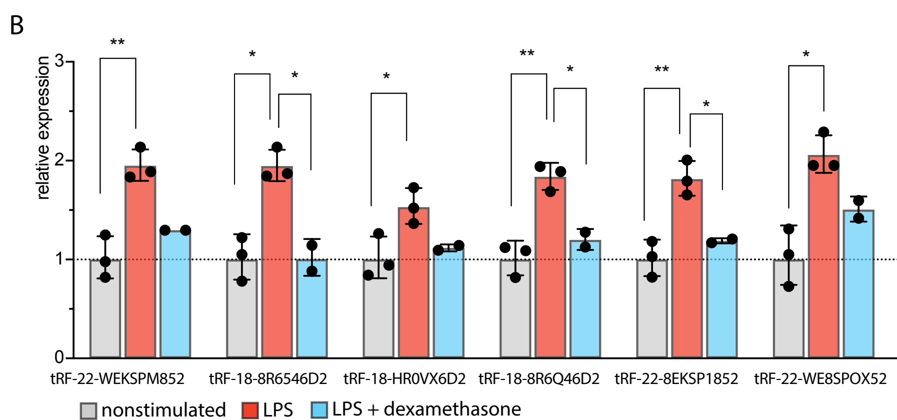
B
relative expression
tRF-22-WEKSPM852
tRF-18-8R6546D2
tRF-18-HR0VX6D2
tRF-18-8R6Q46D2
tRF-22-8EKSP1852
tRF-22-WE8SPOX52
nonstimulated
LPS
LPS + dexamethasone

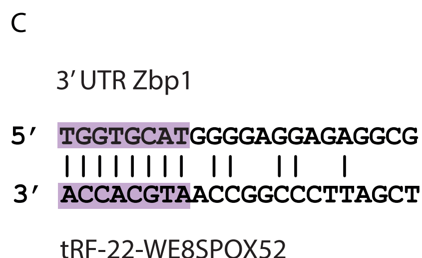
C
3′ UTR Zbp1
5′ TGGTGCATGGGGAGGAGAGGCG
3′ ACCACGTAACCGGCCCTTAGCT
tRF-22-WE8SPOX52

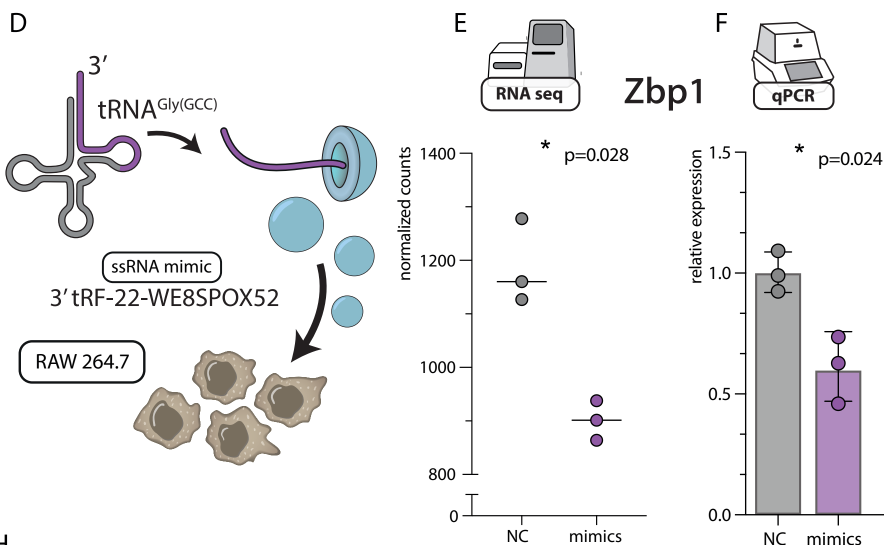
D
3′
tRNA^Gly(GCC)
ssRNA mimic
3′ tRF-22-WE8SPOX52
RAW 264.7
E
RNA seq
Zbp1
F
qPCR
normalized counts
p=0.028
NC
mimics
relative expression
p=0.024

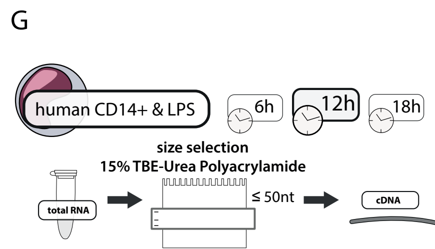
G
human CD14+ & LPS
6h
12h
18h
size selection
15% TBE-Urea Polyacrylamide
total RNA
≤ 50nt
cDNA

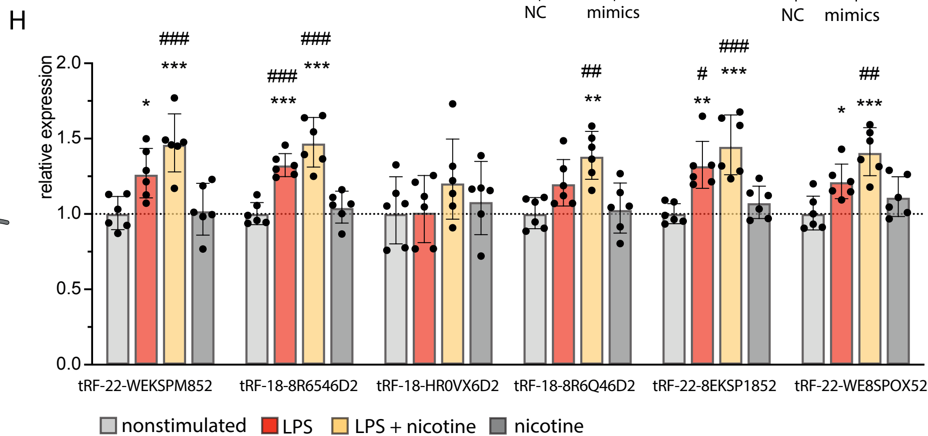
H
relative expression
tRF-22-WEKSPM852
tRF-18-8R6546D2
tRF-18-HR0VX6D2
tRF-18-8R6Q46D2
tRF-22-8EKSP1852
tRF-22-WE8SPOX52
nonstimulated
LPS
LPS + nicotine
nicotine